Supplementary Information

Supplementary data

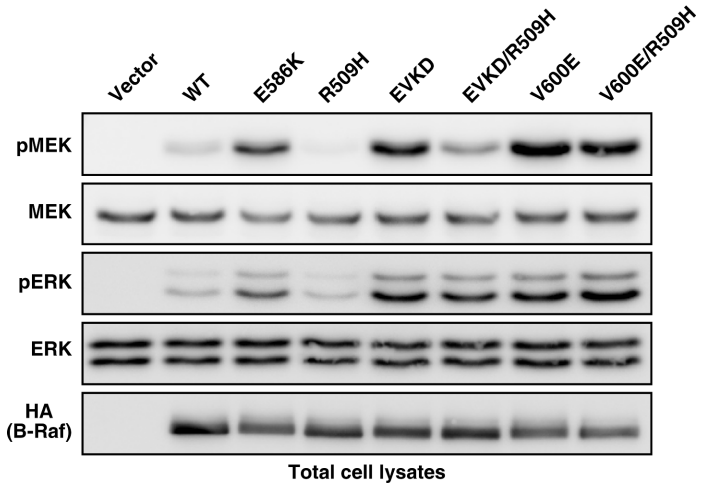

Figure S1 Unlike B-Raf^{wt} and B-Raf^{EVKD}, the MEK phosphorylation potential of B-Raf^{V600E} is hardly affected by the R509H DIF mutation. The indicated HA-tagged B-Raf constructs were expressed in Plat-E cells and analysed by Western blotting of total cell lysates with the indicated antibodies.

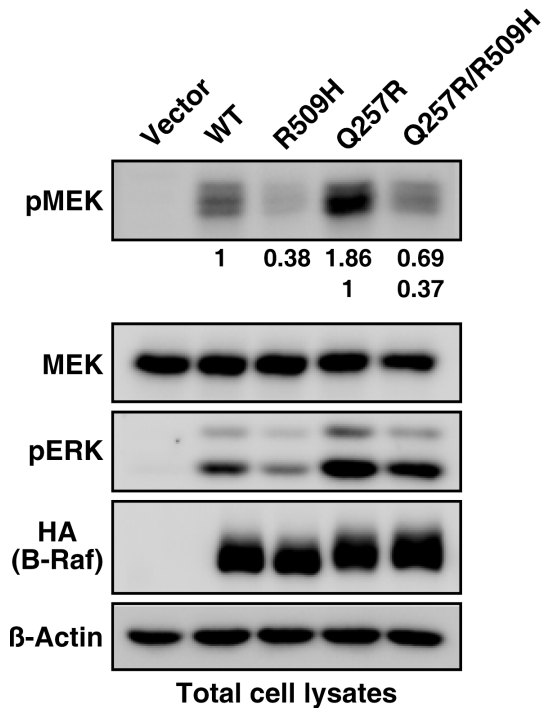

Figure S2 B-Raf^{wt} and B-Raf^{Q257R} are similarly affected by the R509H DIF mutation. The indicated HA-tagged B-Raf constructs were expressed in Plat-E cells and analysed by Western blotting of total cell lysates with the indicated antibodies. Shown values represent the MEK phosphorylation potential of the respective HA-B-Raf protein relative to B-Raf^{wt} (top) or B-Raf^{Q257R} (bottom).

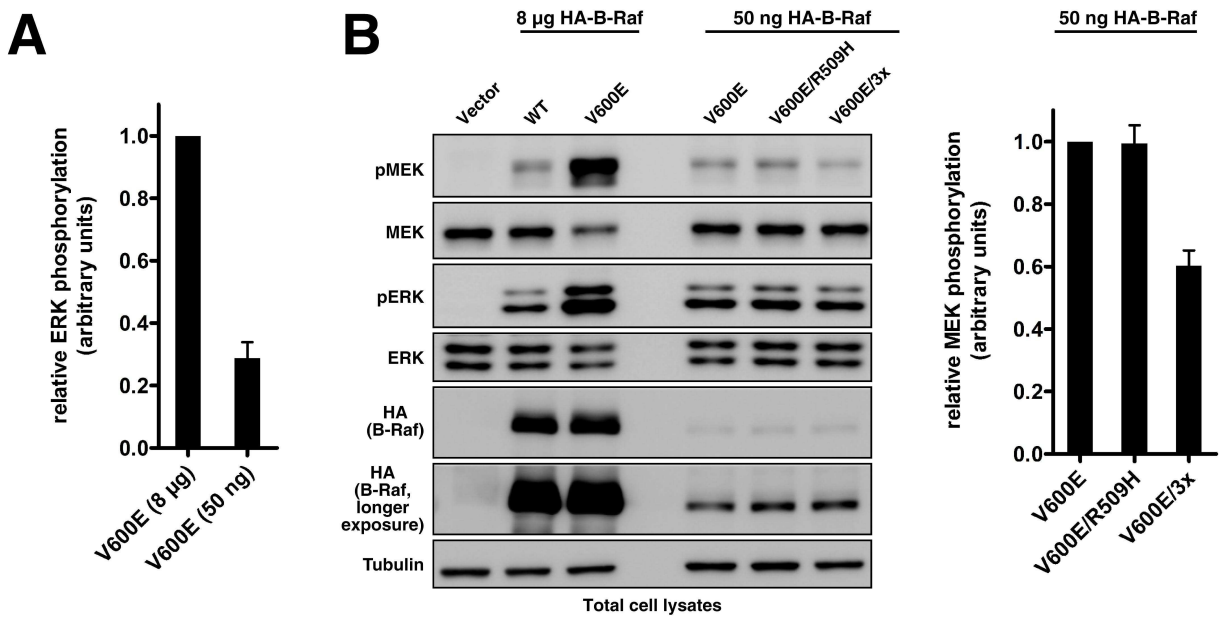

Figure S3 The minor impact of DIF mutations on the B-Raf^{V600E} MEK phosphorylation potential is not based on saturation of the experimental system. **(A)** Bar graph showing the relative levels of ERK phosphorylation after transfecting 8 µg or 50 ng of the pMIG/HAh*BRAF*^{V600E} construct. Shown data represent the mean ± S.E.M. from five independent transfections (normalised on tubulin). **(B)** The indicated HA-tagged B-Raf constructs were expressed in Plat-E cells and analysed by Western blotting of total cell lysates with the indicated antibodies (left). A bar graph representing the mean MEK phosphorylation differential between B-Raf^{V600E}, B-Raf$^{V600E/R509H}$ and B-Raf$^{V600E/3x}$ ± S.E.M. from five independent transfections (normalised on HA-B-Raf) is shown on the right. Please note that each 50 ng HA-B-Raf DNA reaction was supplemented with 7.95 µg empty vector DNA to ensure equal amounts of total DNA per transfection.

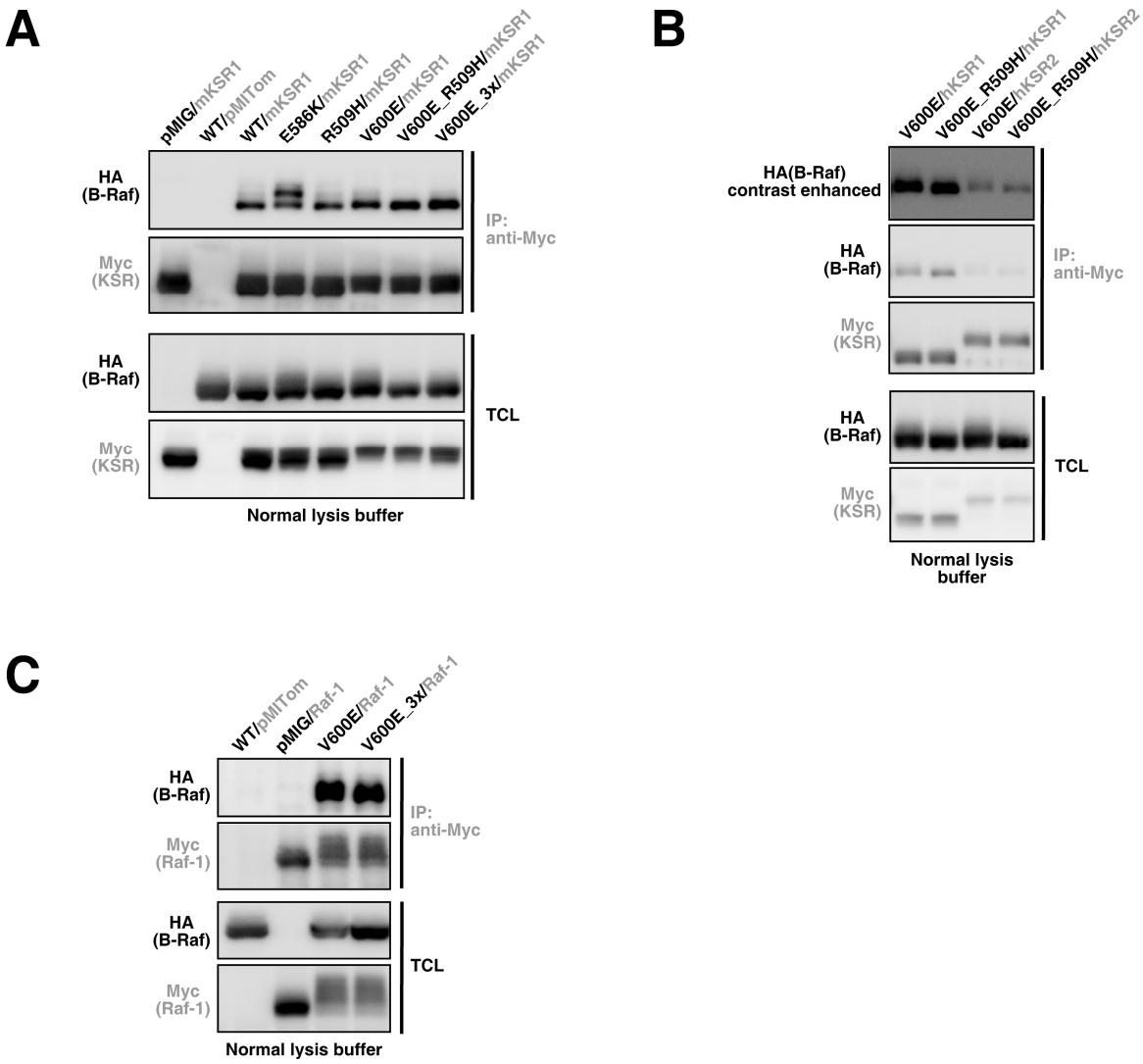

Figure S4 The DIF is not required for B-Raf^{V600E} hetero-dimerisation with Raf-1 or KSR proteins. (**A**)-(**C**) The indicated HA- or Myc-tagged B-Raf constructs were co-expressed in Plat-E cells as described for Figure 3A and B and purified with anti-Myc antibodies. Immunecomplexes and total cell lysates (TCL) were analysed by Western blotting with the indicated antibodies.

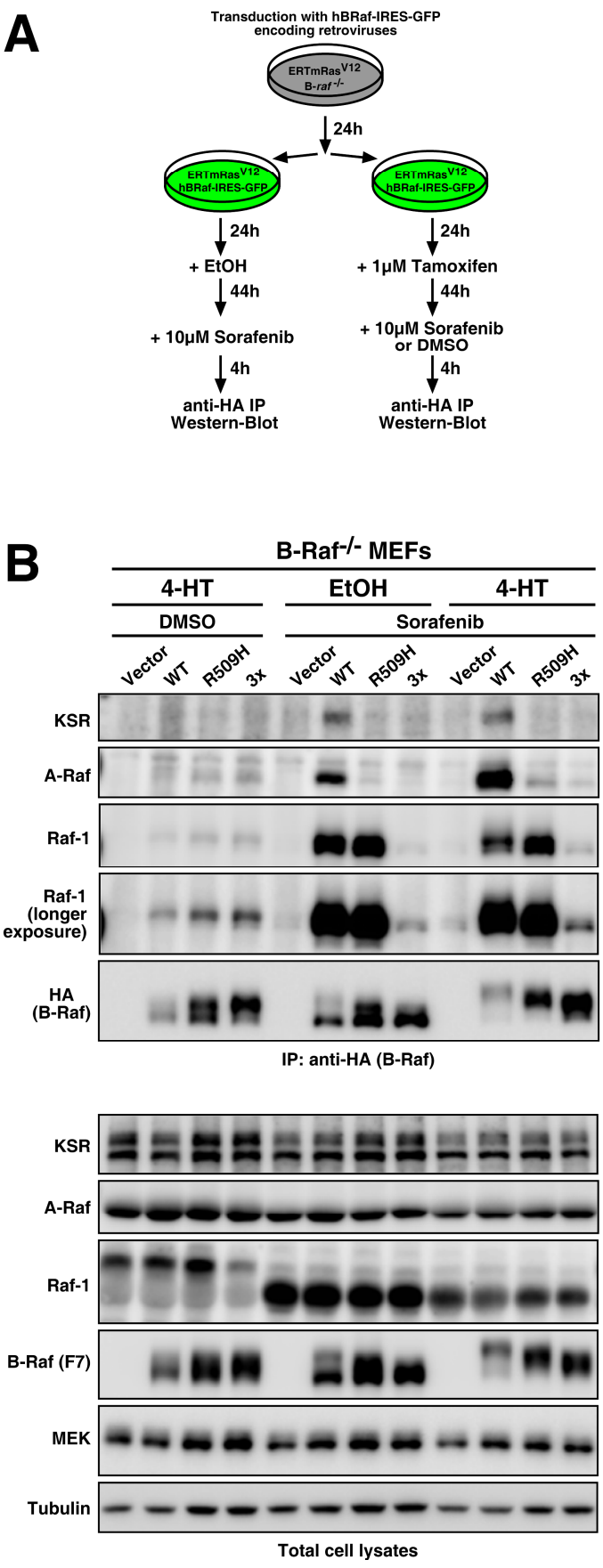

Figure S5 Raf protein complex formation upon sorafenib treatment is DIF-dependent. **(A)** Workflow for complementation of B-Raf deficient MEFs with retroviral B-Raf expression vectors, subsequent release of oncogenic Ras^{V12} (see 6A for details) and treatment with 10 µM sorafenib or vehicle (DMSO) for 4 h. **(B)** The indicated HA-B-Raf constructs were expressed in the MEFs described in (6A/7A) and purified with anti-HA (3F10) antibodies from normal lysis buffer (NLB) lysates. Prior to lysis, the MEFs were treated with 4-HT or vehicle (EtOH) followed by sorafenib or vehicle (DMSO) for 4 h. Immune-complexes were analysed by Western blotting with the indicated antibodies.

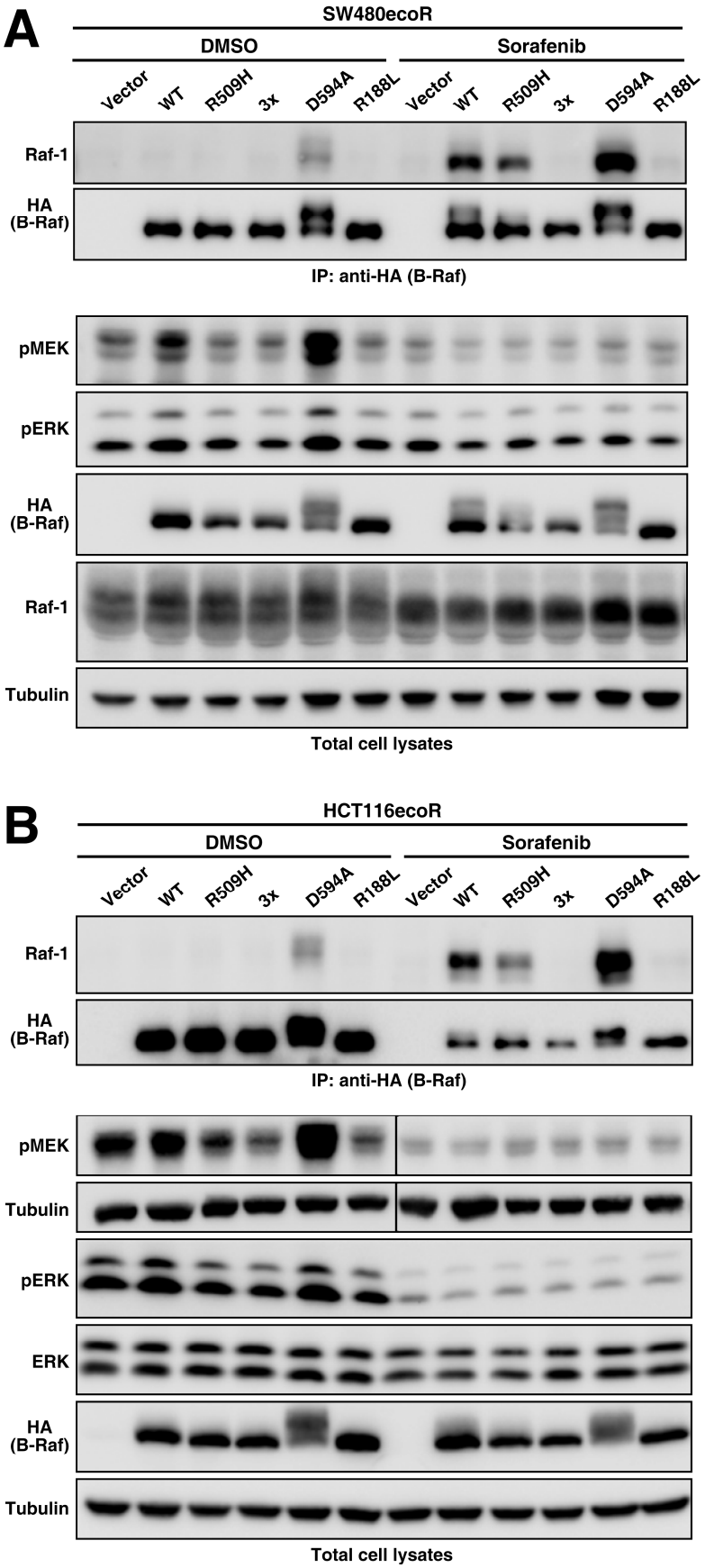

Figure S6 Raf protein complex formation upon sorafenib treatment in human cancer cell lines is DIF-dependent. The indicated HA-B-Raf constructs were expressed in **(A)** SW480ecoR or **(B)** HCT116ecoR cells and purified with anti-HA (3F10) antibodies after DMSO (vehicle control) or sorafenib (10 μM) treatment for 4 h. Immunecomplexes were analysed by Western blotting with the indicated antibodies. Please note that the pMEK as well as the upper tubulin blot in (B) have been sliced as indicated.

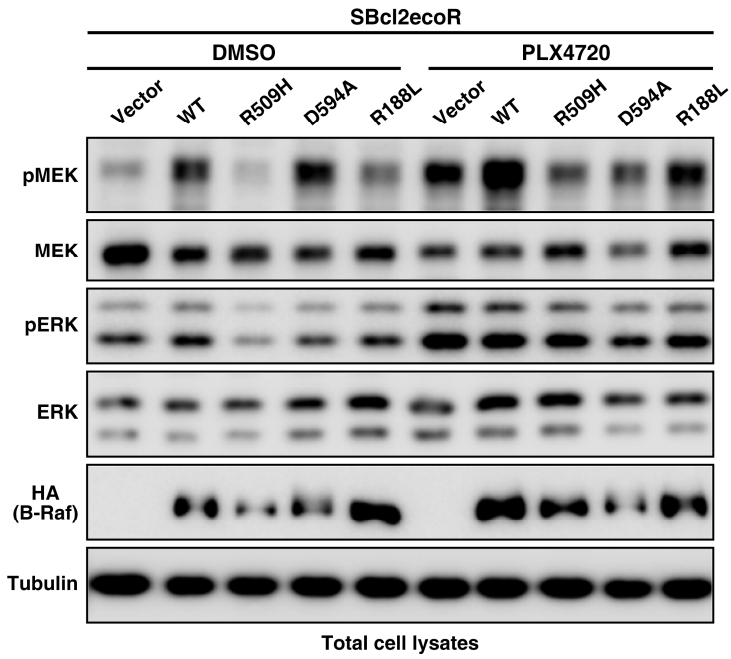

Figure S7 Ectopic expression of B-Raf^{R509H} suppresses PLX4720-induced paradoxical MEK/ERK activation in the human *NRAS*^{Q61K}-mutant melanoma cell line SBcl2. The indicated HA-tagged B-Raf constructs were transduced into SBcl2 cells transiently expressing an ecotropic receptor (SBcl2ecoR) facilitating infections with murine retroviruses. Please see supplementary methods for details. Following treatment with DMSO (vehicle) or 1 µM PLX4720 for 4 h, total cell lysates were analysed by Western blotting with the indicated antibodies. Please note that despite the lower expression levels of B-Raf^{R509H} compared to B-Raf^{wt}, the former already possesses sufficient dominant-negative activity to decrease the resulting levels of MEK/ERK phosphorylation below those of the vector control.

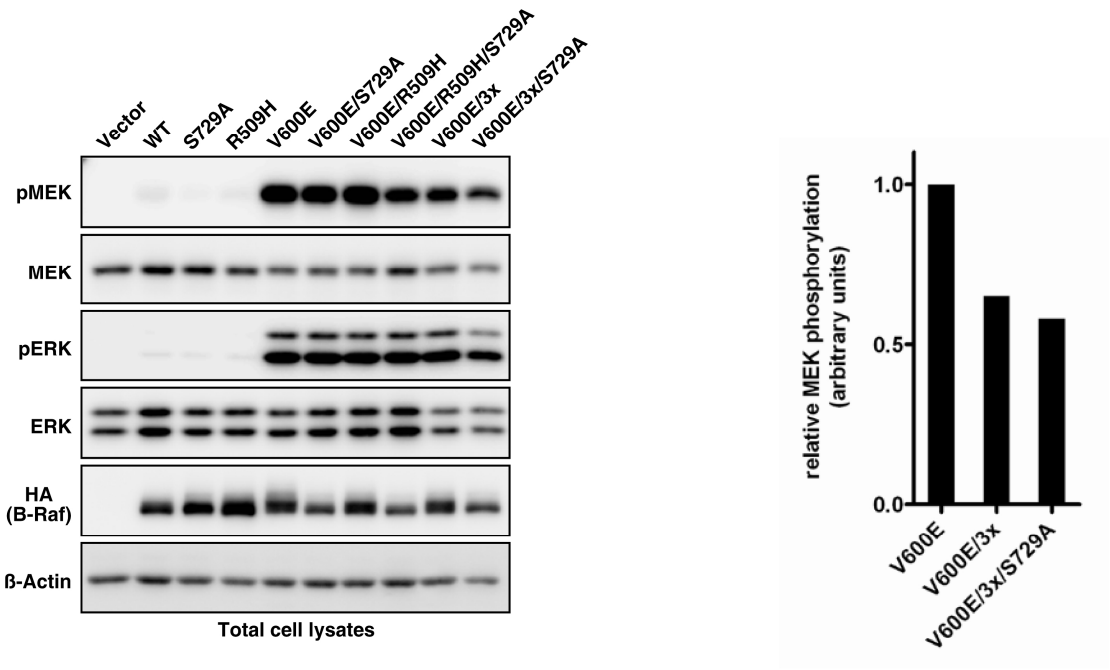

Figure S8 B-Raf^{V600E} proteins lacking both an intact DIF and the C-terminal 14-3-3 binding site S729 still represent strong MEK/ERK pathway activators. The indicated HA-B-Raf constructs were expressed in Plat-E cells and total cell lysates were analysed by Western blotting with the indicated antibodies (left). A bar graph displaying the MEK phosphorylation levels induced by B-Raf^{V600E}, B-Raf$^{V600E/3x}$ and B-Raf$^{V600E/3x/S729A}$ is shown on the right. The chemiluminescence signal elicited by B-Raf^{V600E} was set to 100% including normalization for HA-B-Raf expression.

Supplementary Tables

Table S1 Description of the human B-Raf proteins used in this study.

Mutation	Properties	References
R188L	Abrogation of Ras/Raf interaction	(Brummer et al., 2006a; Brummer et al., 2002; Marais et al., 1997)
Q257R	Believed to counteract auto-inhibitory potential of the CR1, found in cardio-facial-cutaneous syndrome	(Niihori et al., 2006)
S365A	Devoid of 14-3-3 binding to the N-terminus of B-Raf, mimics upstream activation	(Brummer et al., 2006a)
G469A	Glycine of the glycine-rich P-loop replaced by alanine, assumed to disturb the inactive conformation by disrupting the V600 – F468 interaction	(Davies et al., 2002; Ritt et al., 2010; Wan et al., 2004)
R509H	Dimer interface mutation, described to abrogate dimer formation of D-Raf kinase domains	(Rajakulendran et al., 2009)
L515G	Dimer interface mutation, described to abrogate dimer formation of D-Raf kinase domains	(Rajakulendran et al., 2009)
M517W	Dimer interface mutation, described to abrogate dimer formation of D-Raf kinase domains	(Rajakulendran et al., 2009)
3x	Combined mutation of R509H, L515G and M517W	this study
E586K	Increased dimerisation capacity, found in human tumours	(Emuss et al., 2005; Rajakulendran et al., 2009)
insT	Insertion of threonine (TVKS → TTVKS) within the activation loop, shown to be hyperactive and found in pilocytic astrocytoma	(Eisenhardt et al., 2011)
D594A	Catalytically inactive due to alanine substitution of the critical D594 residue of the DFG-motif	Heidorn et al., 2010
V600E	Valine within the activation loop replaced by glutamate (TVKS → TEKS), drives development of a number of human tumors e.g. melanoma, believed to be phospho-mimetic	(Davies et al., 2002; Ritt et al., 2010; Wan et al., 2004)
EVKD	Phospho-acceptor sites within the activation loop replaced by constitutively charged glutamate and aspartate residues (TVKS→ EVKD), hyperactive	(Zhang and Guan, 2000)
S729A	Devoid of 14-3-3 binding to the C-terminus of B-Raf	(Brummer et al., 2006a; Fischer et al., 2009; MacNicol et al., 2000)
CAAX	Carries the polybasic region and isoprenylation motif of K-Ras at its C-terminus, constitutively tethered to the membrane and hyperactive	(Papin et al., 1998)

Table S2 Quantification of pMEK levels in Figures 1-6.
Paired one- or two-tailed Student's t-tests were performed using the TTEST function of Microsoft Excel. All samples were normalised to HA-B-Raf [TCLs] or Myc-B-Raf/Raf-1 [(Co-)IPs] and tested against the wild-type Raf protein(s), except for Figure 1G.

Figure 1G			**One-tailed**
	Mean	**S.E.M.**	**p-value**
WT	1.000	0	**WT**
R509H	0.375	0.0440	0.000016
3x	0.056	0.0050	0.000014
S365A	1.000	0.0000	**S365A**
S365A/R509H	0.310	0.0143	0.000216
E586K	1.000	0.0000	**E586K**
E586K/R509H	0.263	0.041	0.001508
EVKD	1.000	0.0000	**EVKD**
EVKD/R509H	0.408	0.0199	0.000004
EVKD/3x	0.147	0.0356	0.000868
CAAX	1.000	0.0000	**CAAX**
CAAX/R509H	0.160	0.020	0.000283
V600E	1.000	0.0000	**V600E**
V600E/R509H	0.861	0.0355	0.008665
V600E/3x	0.544	0.0337	0.002720
G469A	1.000	0.0000	**G469A**
G469A/R509H	0.610	0.0896	0.024485
insT	1.000	0.0000	**insT**
insT/R509H	0.867	0.022	0.012919

Figure 3B			**Two-tailed**
	Mean	**S.E.M.**	**p-value**
WT_WT	1.0000	0	**WT/WT**
R509H_WT	0.1934	0.0616	0.000001
V600E_V600E	3.1651	0.3967	0.000278
V600E/R509H_V600E	0.2316	0.0508	3.2259E-08
V600E/3x_V600E	0.1906	0.0362	9.00433E-08
WT_V600E	1.3336	0.1458	0.055959

Figure 3C			**One-tailed**
	Mean	**S.E.M.**	**p-value**
WT_WT	1	0	**WT/WT**
R509H_WT	0.4033	0.1093	0.015976
G469A/G469A	3.1033	0.1501	0.002529
G469A/R509H_G469A	0.5200	0.1704	0.053148

Figure 6C			**One-tailed**
	Mean	**S.E.M.**	**p-value**
EV	0.3433	0.0145	0.000245
WT	1.0000	0	**WT**
R509H	0.2767	0.0762	0.005462
D594A	2.3100	0.4588	0.051955
D594A/R509H	0.2867	0.0775	0.005804

Figure 6D			**One-tailed**
	Mean	**S.E.M.**	**p-value**
WT_Raf-1	1	0	**WT/Raf-1**
R509H_Raf-1	0.9367	0.0353	0.107223
D594A_Raf-1	2.5367	0.9900	0.130400
D594A/R509H_Raf-1	1.5400	0.6213	0.238205

Figure 6E			**One-tailed**
	Mean	**S.E.M.**	**p-value**
Raf-1^{wt}_Raf-1^{wt}	1	0	**WT/Raf-1**
Raf-1^{R401H}_Raf-1^{wt}	1.0700	0.1415	0.6699

Figure 6F			**One-tailed**
	Mean	**S.E.M.**	**p-value**
K-Ras^{G12V}_EV	1	0	**K-Ras^{G12V}_EV**
EV_Raf-1^{wt}	5.1905	1.0708	0.0016
K-Ras^{G12V}_ Raf-1^{wt}	0.4518	0.0738	0.0595
K-Ras^{G12V}_ Raf-1^{R401H}	0.1015	0.0362	0.0177

Supplementary Methods

Retrieval of Raf protein sequences and their alignments

Sequence alignments were performed using the MegAlign software and the Clustal method with PAM100 residue weight table. The following sequences were used (with accession numbers in brackets): human B-Raf (*Homo sapiens*; M95712), murine B-Raf (*Mus musculus*; NP_647455), Opossum B-Raf (*Monodelphis domestica;* XP_001375430), Platypus B-Raf (*Ornithorhynchus anatinus*; XP_001516512), chicken B-Raf (*Gallus gallus*; NP_990633), African clawed frog B-Raf (*Xenopus laevis*; AAU29410), Zebrafish B-Raf (*Danio rerio*; CAH69043), puffer fish B-Raf (*Takifugu rubripes*; NP_001032957), sea urchin Raf (*Strongylocentrotus lividus*; XP_781094), giant owl limpet (*Lottia gigantea*; gw1.24.168.1), D-Raf/Pole Hole (*Drosophila melanogaster*; NP_525047), LIN-45 (*Caenorhabditis elegans*; NM_171367), sea anemone Raf (*Nematostella vectensis*; XP_001639152), *Trichoplax* Raf (*Trichoplax adhaerens* ; XP_002112616), murine Ksr1 (*Mus musculus*; NP_038599.1) and fruit fly Ksr (*Drosophila melanogaster*; NP_524236.2)

Cell lines and their cultivation and trans- or infection

The propagation of Plat-E cells, a kind gift of Dr. Kitamura, has been described previously (Morita et al., 2000). For transfection of Plat-E cells, DNA was mixed with PEI in a ratio of 1:3 in plain DMEM and the mixture was allowed to rest for 20 min before adding it to the cells. For virus preparation, the Plat-E supernatant was filtered with a 0.22 µm Millipore filter and complemented with polybrene to a final concentration of 8 µg/ml to reduce cell surface charges. Twenty-four hours before retroviral infection, cells were plated in 10 cm dishes and lysed after another 48 h.

The DT40 cell line allowing the 4-hydroxy-tamoxifen (4-HT) inducible deletion of the chicken c-*mil*/*raf*-1 and c-R*mil*/B-*raf* genes, DT40MCM/raf-1^{flE3}/B-raf^{flE6} (DT40^{floxRaf} in short) and its cultivation has been described in detail (Brummer et al., 2002). In brief, this cell line is derived from DT40MCM#2 cells, which constitutively express the 4-HT inducible Cre-recombinase MerCreMer (Brummer et al., 2003), and has been modified by multiple rounds of homologous recombination in that way that the chicken B-*raf* and *raf*-1 can be inactivated by Cre/loxP-mediated recombination (Brummer et al., 2002). In order to facilitate their infection with ecotropic retroviruses, a well-characterised subclone of DT40^{floxRaf}, DK37, was transfected with pQCXIPN/ecoR, a kind gift from Amanda Russell (Garvan Institute, Sydney) encoding the receptor for murine retroviruses (Albritton et al., 1989). Following stable selection with neomycin (2 mg/ml), a pool of DK37ecoR cells was used for the experiments described in Figure 2B and C.

MEFs were cultured in DMEM (4.5 g/l glucose, 10% fetal calf serum (heat inactivated), 2 mM L-glutamine, 10mM HEPES, 200U/ml penicillin, 200µg/ml streptomycin) were incubated under water vapour saturated atmosphere at 37°C and 5% CO_2. MEFs were generated using standard procedures from d13 B-*raf*$^{flox/flox}$ mouse embryos from a mixed C57/Bl6xBalb/C background ((Chen et al., 2006); kindly provided by Drs. Manuela Baccarini (Vienna) and Elias Hobeika/Michael Reth, MPI Freiburg) and immortalised by infection with the pQCXIH/Tag retroviral construct (kindly provided by Ruth Lyons and Dr. Roger J. Daly, Garvan Institute, Sydney) and subsequent selection with hygromycin B (200 µg/ml). Simian Virus 40 large T antigen (Tag) positive MEFs, which retained their normal morphology and a proper contact inhibition response were selected for further studies. In order to inactivate the B-*raf* locus in the MEFs, they were infected with a Kozak-optimized pMItom-CreERT2 or pBABE-puro-CreERT2 construct (Michael Röring, this study). The coding sequence of CreERT2 (Feil et al., 1996) was kindly provided by Dr. Eva Hug (MPI Freiburg). Infected cells were then sorted by flow cytometry for high tdtomato expression or selected with puromycin (7 µg/ml). Cre activity and subsequent recombination of the B-*raf* locus by excision of the invariant exon 12 was induced by exposure of the MEFs to 4-HT (1 µM). Efficient recombination was confirmed by genomic PCR analyses and Western blotting. Following infection with pBABE-puro-CreERT2, this MEF pool was treated with 4-HT (1 µM) for complete recombination of the B-*raf* locus. Thereafter, these recombined MEFs were super-infected with a retroviral pMItom construct (see expression vector section for details) harbouring the coding sequence of ERTmHRAS^{V12}, which was previously obtained from

Addgene (Cambridge, MA, USA) (Dajee et al., 2002), and then sorted for high tdtomato expression. The indicated pMIG/HAh*BRAF* constructs were introduced by retroviral infections as described previously (Brummer et al., 2006b). In order to analyse anchorage-independent growth of the infected MEF pools, 96-well plates were coated with 50µl of polyHEMA solution (5mg/ml polyHEMA (Sigma) in 95% Ethanol) per well. The ethanol was allowed to evaporate completely by incubating the plate with its lid in place at 37°C in an incubator over night. Before plating of the cells, the polyhema coated wells were washed once with 100 µl PBS. MEFs, in a ratio of 80% non-infected cells and 20% GFP-positive, infected cells were seeded in a volume of 100µl per well in a density of 10 000 cells per well. At day 4 after seeding, 50 µl of the medium were carefully replaced with 50 µl fresh medium. Each construct was done in triplicates and one picture per well was taken at 100x magnification on day 4 and 7.

Caco-2 cells, a kind gift of Dr. Thomas Brabletz (Freiburg), were transfected with *Ahd*I-linearised pWHE 644, which was kindly provided by Dr. Christian Berens (Erlangen). This vector encodes the doxycline-inducible system components rtTA and rtTS (Danke et al., 2010), and allows for selection with puromycine (8 µg/ml). The resulting Caco-2tet cells, a pool stably expressing the rtTA and rtTS, were subsequently transfected with *Ahd*I-linearised pTET/HAhBRAF-IRES-GFP-bsr vectors (Herr et al., 2011) and selected with blasticidine S (5 µg/ml). Matrigel cultures of Caco-2 cells were set-up as described for MCF-10A cells (Brummer et al., 2006a), except that the aforementioned normal cell culture medium was used in place of the MCF-10A medium.

HT29 and HCT116 cells, both kind gifts of Dr. Thomas Brabletz (Freiburg), were cultured in DMEM medium containing 10% FCS. HT29 cells were infected with pTRIPZ lentiviral constructs according to the protocol of the manufacturer (Open Biosystems) and pools were selected in the presence of puromycine (3 µg/ml). HCT116 and SW480 cells, kindly provided by Dr. Roger Daly and Ms Gillian Lehrbach (Garvan Institute Sydney), were transfected with 2.3 µg *Ssp*I-linearised pQCXIPN/ecoR using an Amaxa nucleofector device (Cell Line Nucleofector™ Kit T, Program L-24. Following stable selection with neomycin (600 µg/ml G418), a pool of neomycin resistant cells was infected with pMIG retroviruses, expanded for 4 days, treated for 4h with Sorafenib (10 µM) and processed to total cell lysates.

SBcl2 cells were kindly provided by Dr. Meenhard Herlyn (Philadelphia) *via* Dr. Georg Häcker (Freiburg) and were cultivated as described previously (Weber et al., 2010). SBcl2 cells were transfected with 3µg circular pQCXIPN/ecoR plasmid DNA using the Amaxa nucleofector device (Cell Line Nucleofector™ Kit V, Program T-020) and infected with pMIG retroviruses 48h later. The infection was repeated the next day and following another 3 days of expansion cells were treated with 1 µM PLX4720 or DMSO, respectively.

Expression vectors

The expression vector pMIG/HAh*BRAF*, which encodes HA-tagged B-Raf (Figure 1A) was derived from pMIG/*BRAF*^{V600E}-Myc/His (a kind gift from Dr. Alexander Swarbrick, Cancer

Research program, Garvan Institute, Sydney) with standard molecular biology methods. In brief, a PCR was performed on pMIG/BRAF^{V600E}-Myc/His with the oligonucleotides *Sal*Ih*BRAF*HAtag (5'-GTCGACC*ATGGCTTCTAGCTATCCTTATGACGTGCCTGACTATGCCAGCCTGGGAGGACCT*ATGGCGGCGCTGAGCGGTGGCGGTGGTGGCGGCGCGGAG-3') and *Sal*Ih*BRAF*STOP (5'-GTCGACTCAGTGGACAGGAAACGCACCATATCCCCCTGCCTG-3') to amplify the *BRAF* cDNA from position 62 to 2359 according to the GenBank deposit of human *BRAF* (accession number M95712.2). The oligonucleotide sequence complimentary to human *BRAF* is underlined. The former oligonucleotide introduces a *Sal*I site, a Kozak sequence and an N-terminal HA-tag (coding sequence in *italics*) in front of the original start codon, while the latter introduces a STOP codon and a *Sal*I site and removes the original C-terminal Myc/His-tag. The resulting PCR amplicon was subcloned into pBSSK+ and subsequently recovered by *Sal*I digestion and subcloned into *Xho*I-linearised pMIG (Brummer et al., 2006b). The reversal of the V600E mutation and the subsequent introduction of other mutations were performed with standard site-directed mutagenesis techniques. Oligonucleotide sequences are available on request.

In order to generate an expression vector allowing the doxycycline inducible expression of HAhB-Raf, the HAh*BRAF*-IRES-GFP cassette from the aforementioned pMIG constructs were amplified by PCR using oligonucleotides matching to regions 5' and 3' of this cassette and the proof-reading Phusion polymerase (New England Biolabs). These oligonucleotides introduce each a *Not*I site into the PCR amplicon. The PCR amplicons were then subcloned into the cloning vectors pBSSK+ or pSC-A (both purchased from Stratagene) for further propagation. The subcloned amplicon was then recovered by *Not*I digestion and subcloned into *Not*I-linearised pTET-bsr to yield pTET-on/HAhBRAF-IRES-GFP-bsr. The pTET-bsr vector (Herr et al., 2011), contains a basal promotor and six tet-repressor/inducer binding elements and a *lox*P-flanked blasticidine s resistance (bsr) cassette derived from pA*lox*P-bsr (Arakawa et al., 2001).

In order to generate expression vectors for Myc-tagged KSR proteins, full-length cDNAs for hKSR1 (BC167812) and mKSR1 (BC168386) were obtained from IMAGENES, Berlin, Germany. A cDNA construct containing hKSR2 (BC127603.1) was kindly provided by Dr. Sam Aparicio, Terry Fox Laboratories, Vancouver, Canada. Using Phusion polymerase and oligonucleotides introducing an N-terminal Myc-tag extension (MASEQKLISEEDL) and *Sal*I sites at both termini, an amplicon was generated by PCR and subcloned into the cloning vector pSC-A (Stratagene). Subsequently, these modified cDNAs were excised by *Sal*I digestion and subcloned into the *Xho*I-linearised retroviral expression vector pMITom, a kind gift from Dr. Sebastian Herzog, ZBSA, Freiburg, Germany (Herzog et al., 2008). The pMIberry expression vector was generated in this study by cloning PCR amplified *Nco*I-DsRedExpress2-*Cla*I into the *Nco*I/*Cla*I linearised pMItom vector. This replaced tdtomato with DsRedExpress2, which was previously obtained from Addgene, Cambridge, MA, USA.

In order to generate expression vectors for Myc-tagged human Raf-1, its full-length cDNA present in pCMV/c-Raf (Brummer et al. 2002) was amplified by PCR using Phusion polymerase and oligonucleotides introducing an N-terminal Myc-tag extension (MASEQKLISEEDL) and a *BamH*I and *Xho*I site at the 5' and 3' end, respectively. Subsequently, this modified Raf-1 cDNAs was subcloned into the *BamH*I/*Xho*I-linearised pMIBerry. The pMIG/HAhRaf-1 expression vector was generated by amplifying the human Raf-1 coding sequence in the aforementioned pMIBerry/Myc-hRaf-1 construct with oligonucleotides introducing an N-terminal HA-tag replacing the Myc-tag: *Bam*HI HAhRaf-1 fwd (5'-ATGGATCCACCATGGCTTCTAGCTATCCTTATGACGTGCCTGACTATGCCAGCCTGGGAGGACCTATGGAGCACATACAGGGAGCTTGGAAGACGATCAGCAATGGTTTTGG-3') and *Eco*RI hRaf-1 Stop rev (5'-ATATGAATTCCTAGAAGACAGGCAGCCTCGGGGACGTGG-3'). The oligonucleotide sequence complimentary to human *RAF1* is underlined. Subsequently, the resulting PCR fragment was ligated into the pSC-A vector (Stratagene) and subcloned performing a *Bam*HI/*Eco*RI digest into the *Bgl*II/*Eco*RI linearized pMIG vector. All constructs were confirmed by DNA sequencing. Oligonucleotide sequences and detailed cloning procedures are available on request. The ERTmHRAS^{V12} coding sequence (Dajee et al., 2002) was obtained from Addgene (Cambridge, MA, USA) and subsequently cloned into the pMItom vector. For the construction of a V600E-specific shRNAmir construct, complementary oligonucleotides (V600ETRIPZ3s: 5'gctcgagaaggtatattgctgttgacagtgagcgcagctacagagaaatctcgatgtagtgaagccacagatgtacatcgagatttctctgtagctatgcctactgcctcggatgcctactgcctcggaattca-3'; V600ETRIPZ3as: 5'-tgaattccgaggcagtaggcatccgaggcagtaggcatagctacagagaaatctcgatgtacatctgtggcttcactacatcgagatttctctgtagctgcgctcactgtcaacagcaatataccttctcgagc-3') were annealed and directly digested with *Xho*I and *EcoR*I. The resulting doublestranded DNA was directly subcloned into the *Xho*I/*EcoR*I digested pTRIPZ vector (Open Biosystems).

Kinase assays

A subconfluent 10 cm dish of Plat-E cells was transfected with 8 µg of the indicated pMIG plasmids as described in supplementary data. The cells were lysed in 1 ml NLB 48 h post transfection. Subsequently, 0.5-1 µg rat anti-HA antibody 3F10 was added to 1 ml cleared TCL for 1 h and then incubated with 50 ml Protein G-Sepharose slurry for 3 h. Following six washes with 1ml NLB and three washes with 1ml Kinase assay buffer (KAB; 20mM 4-morpholinepropanesulfonic acid (MOPS), pH 7.2; 25mM β-glycerol phosphate; 5mM EGTA, 1mM sodium orthovanadate, 1mM dithiothreitol), the beads were resuspended in 100 µl KAB. Then, 10 µl of this suspension were mixed with 1 µg recombinant GST-MEK1 and 5 mM ATP in 38 µl KAB as described previously (Brummer et al., 2006a; Eisenhardt et al., 2011). GST-MEK1 was expressed in *E. coli* Rosetta cells and purified as described previously (Brummer et al., 2006a). The IVK reaction was incubated at 30°C for 30 min and

immediately stopped by addition of sample buffer and boiling for 5 min. Subsequently, the reactions were separated by SDS–PAGE and blotted with phospho-MEK antibodies as a read-out for the MEK kinase activity of the purified HA-B-Raf proteins. Following subtraction of the background signal (kinase assay reaction performed with anti-HA immunoprecipitates of empty vector-transfected cells), the relative, specific B-Raf activity was determined by division of each activity by that of B-Raf^{wt}.

BN-PAGE analysis

The day prior to transfections, 2,5 x 10^6 cells were plated and transfected with the indicated pMIG/HAhB-Raf constructs as described above. Fourty-eight hours after transfection, cells were lysed in 1 ml of cold BN-lysis buffer (20 mM Bis-Tris, pH 7.0, 500 mM ε-amino caproic acid, 20 mM NaCl, 2 mM EDTA, and 10% glycerol) supplemented with 0.1% Triton X-100, protease inhibitors (protease inhibitor cocktail P2714 from Sigma-Aldrich, 1 mM PMSF) and phosphatase inhibitors (0.5 mM NaF, 1mM Na_3VO_4). Alternatively, HT29 cells were plated (1x10^5 cells per 6-well) and induced with 2 µg/ml doxycyline 24 h later. Four days after induction, the cells were lysed as described for Plat-E cells. After incubation on ice for 20 min, the lysate was centrifuged at 13,000*g* at 4°C for 10 min. The supernatant was removed and stored on ice for the following steps. Thereafter, 200 µl of supernatant were dialyzed against 20 ml cold BN-lysis buffer supplemented with 0.1% Triton X-100, protease inhibitor (1 mM PMSF) and phosphatase inhibitor (1 mM Na_3VO_4) at 4°C for at least 6 h as described previously (Swamy et al., 2006).

BN gels of a 5-9% gradient were prepared as described (Schagger et al., 1994; Swamy et al., 2006). Ten µg of ferritin (440 and 880 kDa, from Sigma-Aldrich) and 10 µl of high molecular weight calibration kit for native electrophoresis (GE Healthcare, UK) were used as marker. One to10 µl of dialysed supernatant was loaded on the BN gel and overlaid with blue cathode buffer. No sample buffer was added to the samples before loading. The BN gel run was performed overnight at 4°C using blue cathode buffer (50 mM Tricine, 15 mM Bis-tris, pH 7.0, 0.02% Coomassie blue G250) and anode buffer (50 mM Bis-tris, pH 7.0). Subsequently, BN-PAGE separated proteins were blotted onto PVDF membranes by Semi-Dry Transfer. An additional 0.02% of SDS was added to the standard transfer buffer.

RT-PCR analysis

HT29 cells were plated (1x10^5 cells per 6-well) and induced with 2 µg/ml doxycyline 24 h later. Four days after induction, RNA was isolated using the RNeasy Plus Mini Kit (Qiagen). First strand cDNA was synthesized using the Revert Aid Kit (Fermentas). Primers specific to exon 13 (5`-attgttacccagtggtgtgagggctccagc-3') and exon 16 (5'-gctgtatggatttttatcttgcattctgat-3') of *BRAF* were used to amplify exon 15 that encodes the TV^{600}KS-motif. The PCR amplicon was extracted after gel electrophoresis and the presence of the wildtype TVKS motif or the mutated TEKS motif was assessed by sequencing (GATC Biotech AG, Konstanz, Germany).

Protein structure analysis

Protein structure analysis was performed using MacPyMol v1.3 (The PyMOL Molecular Graphics System, Version 1.3, Schrödinger, LLC). Structural co-ordinates were obtained from X-ray crystal structures of the kinase domains of human B-Raf^{wt} (1uwh) and B-Raf^{V600E} (1uwj) in complex with BAY 439006 inhibitor (sorafenib; (Wan et al., 2004)). For comparison, the structure of B-Raf^{V600E} (3og7) is also shown in complex with PLX4032 inhibitor (Bollag et al., 2010). To map dimer contacts in wt and mutant B-Raf, we used Pymol to find surface accessible atoms within 5 Å of the adjacent protomer in each crystal structure. Additional analysis of DIFs, including calculation of interface surface area, was performed using the PISA server at the European Bioinformatics Institute (EBI) (http://www.ebi.ac.uk/msd-srv/prot_int/pistart.html).

Statistical analyses

Paired one- or two-tailed Student's t-test were used after normalisation to identify significant experimental factors such as mutations in B-Raf. Statistical calculations were performed using the VBA statistics toolkit of Microsoft Excel 2007.

Supplementary References

Albritton, L. M., Tseng, L., Scadden, D., and Cunningham, J. M. (1989). A putative murine ecotropic retrovirus receptor gene encodes a multiple membrane-spanning protein and confers susceptibility to virus infection. Cell *57*, 659-666.

Arakawa, H., Lodygin, D., and Buerstedde, J. M. (2001). Mutant loxP vectors for selectable marker recycle and conditional knock-outs. BMC Biotechnol *1*, 7.

Bollag, G., Hirth, P., Tsai, J., Zhang, J., Ibrahim, P. N., Cho, H., Spevak, W., Zhang, C., Zhang, Y., Habets, G., *et al.* (2010). Clinical efficacy of a RAF inhibitor needs broad target blockade in BRAF-mutant melanoma. Nature *467*, 596-599.

Brummer, T., Martin, P., Herzog, S., Misawa, Y., Daly, R., and Reth, M. (2006a). Functional analysis of the regulatory requirements of B-Raf and the B-Raf(V600E) oncoprotein. Oncogene *25*, 6262-6276.

Brummer, T., Naegele, H., Reth, M., and Misawa, Y. (2003). Identification of novel ERK-mediated feedback phosphorylation sites at the C-terminus of B-Raf. Oncogene *22*, 8823-8834.

Brummer, T., Schramek, D., Hayes, V. M., Bennett, H. L., Caldon, C. E., Musgrove, E. A., and Daly, R. J. (2006b). Increased proliferation and altered growth factor dependence of human mammary epithelial cells overexpressing the Gab2 docking protein. J Biol Chem *281*, 626-637.

Brummer, T., Shaw, P., Reth, M., and Misawa, Y. (2002). Inducible gene deletion reveals different roles for B-Raf and Raf-1 in B-cell antigen receptor signalling. 11032810 *21*, 5611-5622.

Chen, A. P., Ohno, M., Giese, K. P., Kuhn, R., Chen, R. L., and Silva, A. J. (2006). Forebrain-specific knockout of B-raf kinase leads to deficits in hippocampal long-term potentiation, learning, and memory. J Neurosci Res *83*, 28-38.

Dajee, M., Tarutani, M., Deng, H., Cai, T., and Khavari, P. A. (2002). Epidermal Ras blockade demonstrates spatially localized Ras promotion of proliferation and inhibition of differentiation. Oncogene *21*, 1527-1538.

Danke, C., Grunz, X., Wittmann, J., Schmidt, A., Agha-Mohammadi, S., Kutsch, O., Jack, H. M., Hillen, W., and Berens, C. (2010). Adjusting transgene expression levels in lymphocytes with a set of inducible promoters. J Gene Med *12*, 501-515.

Davies, H., Bignell, G. R., Cox, C., Stephens, P., Edkins, S., and Clegg, S. (2002). Mutations of the BRAF gene in human cancer. Nature *417*, 949-954.

Eisenhardt, A. E., Olbrich, H., Roring, M., Janzarik, W., Anh, T. N., Cin, H., Remke, M., Witt, H., Korshunov, A., Pfister, S. M., *et al.* (2011). Functional characterization of a BRAF insertion mutant associated with pilocytic astrocytoma. Int J Cancer *129*, 2297–2303.

Emuss, V., Garnett, M., Mason, C., and Marais, R. (2005). Mutations of C-RAF are rare in human cancer because C-RAF has a low basal kinase activity compared with B-RAF. Cancer Res *65*, 9719-9726.

Feil, R., Brocard, J., Mascrez, B., LeMeur, M., Metzger, D., and Chambon, P. (1996). Ligand-activated site-specific recombination in mice. Proc Natl Acad Sci U S A *93*, 10887-10890.

Fischer, A., Baljuls, A., Reinders, J., Nekhoroshkova, E., Sibilski, C., Metz, R., Albert, S., Rajalingam, K., Hekman, M., and Rapp, U. R. (2009). Regulation of RAF activity by 14-3-3 proteins: RAF kinases associate functionally with both homo- and heterodimeric forms of 14-3-3 proteins. J Biol Chem *284*, 3183-3194.

Herr, R., Wohrle, F. U., Danke, C., Berens, C., and Brummer, T. (2011). A novel MCF-10A line allowing conditional oncogene expression in 3D culture. Cell Commun Signal *9*, 17.

Herzog, S., Hug, E., Meixlsperger, S., Paik, J. H., DePinho, R. A., Reth, M., and Jumaa, H. (2008). SLP-65 regulates immunoglobulin light chain gene recombination through the PI(3)K-PKB-Foxo pathway. Nat Immunol *9*, 623-631.

MacNicol, M. C., Muslin, A. J., and MacNicol, A. M. (2000). Disruption of the 14-3-3 binding site within the B-Raf kinase domain uncouples catalytic activity from PC12 cell differentiation. J Biol Chem *275*, 3803-3809.

Marais, R., Light, Y., Paterson, H. F., Mason, C. S., and Marshall, C. J. (1997). Differential regulation of Raf-1, A-Raf, and B-Raf by oncogenic ras and tyrosine kinases. J Biol Chem *272*, 4378-4383.

Morita, S., Kojima, T., and Kitamura, T. (2000). Plat-E: an efficient and stable system for transient packaging of retroviruses. Gene Ther *7*, 1063-1066.

Niihori, T., Aoki, Y., Narumi, Y., Neri, G., Cave, H., Verloes, A., Okamoto, N., Hennekam, R. C., Gillessen-Kaesbach, G., Wieczorek, D., *et al.* (2006). Germline KRAS and BRAF mutations in cardio-facio-cutaneous syndrome. Nat Genet *38*, 294-296.

Papin, C., Denouel-Galy, A., Laugier, D., Calothy, G., and Eychene, A. (1998). Modulation of kinase activity and oncogenic properties by alternative splicing reveals a novel regulatory mechanism for B-Raf. J Biol Chem *273*, 24939-24947.

Rajakulendran, T., Sahmi, M., Lefrancois, M., Sicheri, F., and Therrien, M. (2009). A dimerization-dependent mechanism drives RAF catalytic activation. Nature *461*, 542-545.

Ritt, D. A., Monson, D. M., Specht, S. I., and Morrison, D. K. (2010). Impact of feedback phosphorylation and Raf heterodimerization on normal and mutant B-Raf signaling. Mol Cell Biol *30*, 806-819.

Schagger, H., Cramer, W. A., and von Jagow, G. (1994). Analysis of molecular masses and oligomeric states of protein complexes by blue native electrophoresis and isolation of membrane protein complexes by two-dimensional native electrophoresis. Anal Biochem *217*, 220-230.

Swamy, M., Siegers, G. M., Minguet, S., Wollscheid, B., and Schamel, W. W. (2006). Blue native polyacrylamide gel electrophoresis (BN-PAGE) for the identification and analysis of multiprotein complexes. Sci STKE *2006*, pl4.

Wan, P., Garnett, M., Roe, S., Lee, S., Niculescu-Duvaz, D., Good, V., Jones, C., Marshall, C., Springer, C., Barford, D., and Marais, R. (2004). Mechanism of activation of the RAF-ERK signaling pathway by oncogenic mutations of B-RAF. Cell *116*, 855.

Weber, A., Kirejczyk, Z., Besch, R., Potthoff, S., Leverkus, M., and Hacker, G. (2010). Proapoptotic signalling through Toll-like receptor-3 involves TRIF-dependent activation of caspase-8 and is under the control of inhibitor of apoptosis proteins in melanoma cells. Cell Death Differ *17*, 942-951.

Zhang, B. H., and Guan, K. L. (2000). Activation of B-Raf kinase requires phosphorylation of the conserved residues Thr598 and Ser601. Embo J *19*, 5429-5439.